A Small-Angle Scattering Study of Cellulose Whiskers in Aqueous Suspensions

P. Terech,[†] L. Chazeau,[*,‡] and J. Y. Cavaille[‡]

Laboratoire de Physico-Chimie Moléculaire, UMR 5819 CEA-CNRS−Universite J. Fourier, Département de Recherche Fondamentale sur la Matière Condensée, CEA-Grenoble, 17 rue des Martyrs, 38054 Grenoble, Cedex 9, France, and Centre de Recherche sur les Macromolécules Végétales (CNRS), Université Joseph Fourier, B.P. 53 X, F-38041 Grenoble, Cedex 9, France

Received July 7, 1998

ABSTRACT: Fillers with dimensions in the nanometer range are important components of nanocomposites materials. A crucial point for the modeling of the resulting mechanical properties is to determine their average dimensions accurately as is required for the mechanical coupling modeling. In this work, reinforcing particules are cellulose monocrystalline rods with an average length of 1 μm. They are prepared from marine animals and obtained in the form of stable aqueous suspensions. Their precise shape and lateral dimensions are determined by use of the small-angle scattering technique (neutron and X-rays). The study is achieved in a rather extended range of concentration (from 0.071 to 1.37% w/w) within which all scattering patterns are found isotropic and homothetic. A form-factor analysis demonstrates that the whiskers are long and rigid fibers whose cross-sectional shape is rectangular (88 × 182 Å^2). The cross-sectional morphology of the rods is consistent with crystallographic data of the cellulose fillers. The suspensions can be considered as homogeneous in this range of concentration since no significant higher aggregation of the whiskers can be detected.

Introduction

There has been extensive research in the area of polymer fillers to enlarge the versatility of polymer composites. Among all materials used in this context, cellulose presents several advantages such as a reinforcing filler property in composites. Different types of cellulose filler are available, the most simple being the wood fibers, used since decades because of their low cost. Cellulose is biosynthesized as microfibrils whose crystallinity depends on the bioorganism it originates.[1] In our group, particular attention is devoted to the microfibrils synthesized by a marine animal.[2] These microfibrils are found in the envelop of tunicates and exhibit a high crystallinity which is the basis of remarkable mechanical properties. The hydrolysis of these microfibrils yields cellulose whiskers which are quasi-perfect monocrystals.[3] Moreover, the sulfuric acid hydrolysis allows the grafting of sulfate surface groups which stabilize the aqueous whisker suspension by electrostatic repulsion. The typical dimensions of these crystallites lie between 10 and 20 nm diameter for a length of ca. 1 μm. The high interest of such whiskers, in the context of polymer composites, is their large aspect ratio (of about 100) and their high longitudinal modulus (ca. 130−150 GPa[4−7]). Finally, we must point out their high specific surface area (about 150 m^2/g) which could have large consequences on the macroscopic behavior of composite systems in which they constitute the filler. For these reasons, these new fillers have been studied in several matrices (PS-ABu,[2] plasticized PVC[8−11]) and showed, as a result, a strong increase of the mechanical properties of the composites. As an objective to fully analyze the mechanical properties of the new composites, support by a structural investigation of the fillers appears to be a necessary and valuable step. Several works have specifically attempted to determine accurately the cross-sectional features of the cellulose tunicate whisker by transmission electron microscopy (TEM) using microtomes.[12−14] It was shown that the whiskers had two characteristic lateral dimensions across a wide range of values. Although the observed photographs were remarkable, it is necessary to use a complementary and different technique to confirm these results since they were based on the observation of a reduced number of samples prepared using a delicate technique with potential artifacts. The small-angle scattering technique which consists of analyzing the angular distribution of the scattered intensity by a genuine sample (in the presence of its liquid component) is appropriate to complement real-space observations.

Experimental Section

Materials. The cellulose whiskers were obtained from tunicates after a treatment described in Wise et al.[15] The final aqueous suspension neither precipitates nor flocculates due to the electrostatic repulsions between the surface sulfate groups grafted during the sulfuric acid treatment. The whisker D_2O suspension used in neutron scattering experiments was processed by freeze-drying the initial whiskers suspension and then diluting them in D_2O. It has been checked that transmission electron microscopy experiments performed with heavy water suspensions show the same results as do whiskers in light water suspension.

Small-Angle Scattering. Small-angle scattering measurements were performed at the I.L.L. (Grenoble, France) and at the L.L.B. (Saclay, France) reactors for neutron scattering (SANS) and at the L.U.R.E. synchrotron source (Orsay, France) for X-ray scattering (SAXS). Concerning neutron scattering, absolute intensities I were obtained by calibration with the standard scattering of water; SANS data reduction and usual corrections for the detector response and absolute calibration were performed with the standard programs available at the instruments used. All signals being isotropic, a radial averaging of the data was performed. As for elastic scattering conditions, the momentum transfer Q was defined

* To whom correspondence should be addressed.
[†] Laboratoire de Physico-Chimie Moléculaire.
[‡] Centre de Recherche sur les Macromolécules Végétales (CNRS).

10.1021/ma9810621 CCC: $18.00
Published on Web 03/05/1999

Table 1. Whisker Concentration in D_2O Suspensions

sample	WS01	WS02	WS03	WS04	WS05	WS06
concn (% w/w)	1.37	0.91	0.71	0.35	0.18	0.071

Table 2. Values Deduced from the ln(QI) versus Q^2 Plots

sample	slope (Å^2)	radius (Å)	QI_0 (Å^{-1} cm^{-1})	M_l (10^{-20} g/Å)
WS01	1746	84	0.512	1.32
WS02	1701	83	0.379	1.48
WS03	1761	84	0.298	1.48
WS04	1748	84	0.150	1.51
WS05	1825	85	0.078	1.53
WS06	1762	84	0.031	1.55

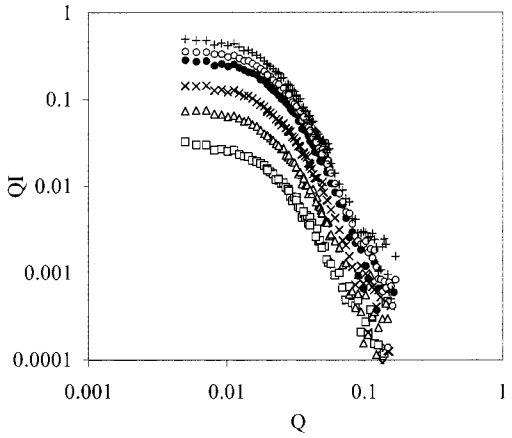

Figure 1. Neutron scattering. QI as a function of Q measured for all the whisker concentrations in D_2O suspensions listed in Table 1: WS01 (+), WS02 (○), WS03 (●), WS04 (×), WS05 (△), WS06 (□). Q is in Å^{-1}, I in cm^{-1}.

as $|Q| = (4\pi/\lambda) \sin \theta$, θ being half the scattering angle and λ the wavelength of the incident beam. The D11 spectrometer of the I.L.L was used at three distances, 1.5, 5, and 20 m with $\lambda = 6$ Å. Two configurations of measurements have been used at the PAXE spectrometer of the L.L.B: detector distances of 5.05 and 2.55 m at respectively $\lambda = 12$ and 6 Å. These experimental conditions provided a [5×10^{-3} Å^{-1}, 2×10^{-1} Å^{-1}] Q-range. In all experiments, a very good overlap of the radially averaged scattering curves obtained with the different configurations was observed. Assuming neat interfaces of the fillers, a constant value was subtracted as an incoherent background scattering from the neutron data. An IQ^4 plot as a function of Q was convenient for its determination since a horizontal plateau at high Q indicates the correct estimation.

Results and Discussion

Six concentrations of whisker suspensions were investigated (cf. Table 1). Figure 1 shows QI versus Q profiles for the six concentrations (LLB data). It appears that the whisker concentration does not influence the shape of the scattering curves, even at low Q. This scattering behavior is a good indication that, in the concentration range studied, there is no significant concentration-dependent aggregation process. Specially, the innermost part of the scattering curves is free of any extra scattering which could indicate the growth of larger aggregates of whiskers when the concentration is increased. Consequently, and considering the high degree of dilution of some of the suspensions, the scattering intensity will be considered in the following as resulting from the form-factor intensity of isolated whiskers.

The experimental scattering curves exhibit all characteristics of a scattering by rodlike particles with a high

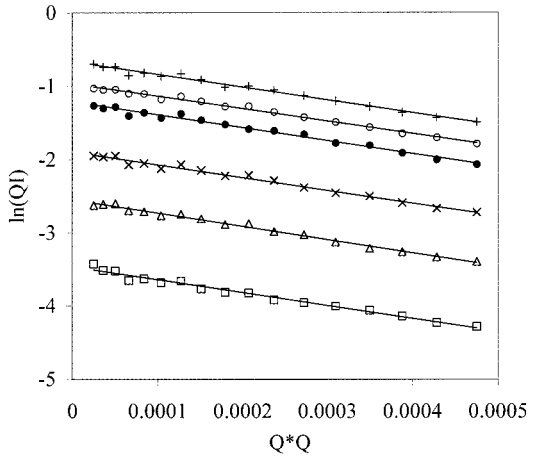

Figure 2. Neutron scattering: ln(QI) versus Q^2 plots for whisker suspensions in D_2O. Same legend as in Figure 1. Q is in Å^{-1}, I in cm^{-1}.

length/diameter ratio. In the case of infinite length cylinders with homogeneous internal structure and without interaction between them, the intensity can be written as[16]

$$I(Q) = \frac{\pi C}{Q}\overline{\Delta b^2} M_L \left[\frac{2J_1(QR_0)}{QR_0}\right]^2 \qquad (1)$$

$J_1(Q)$ is the first-order Bessel function, M_L is the weight by unit length of fiber, C is the concentration (g/cm^3), R_0 is its radius, and $\overline{\Delta b^2}$ is the scattering volumic contrast (in cm g^{-1}). Within a QI versus Q representation, a low-Q plateau characterizes the unidirectional character of rodlike particles (cf. Figure 1). At low QR_0 values ($QR_c < 1$ with $R_c = R_0/\sqrt{2}$ in the case of circular cross section), $I(Q)$ can be expanded as a Gaussian decay:

$$QI(Q) = (QI)_0 \exp\left(-\frac{Q^2 R_0^2}{2}\right) \qquad (2)$$

This decay is apparent in Figure 1. ln(QI) versus Q^2 plots are linear and are used to determine the radius from the slope (eq 2) and the weight per unit length of rods (from the $(QI)_0$ values).

Such plots are shown in Figure 2, and corresponding R_0 and M_l values are collected in Table 2. Values are insensitive to the concentration, confirming the absence of aggregation of the whiskers. The average value of the whisker radius is found to be 84 ± 1 Å while the average weight by unit length M_l is about 1.45×10^{-20} ($\pm 10\%$) g/Å.

An estimation of the radius of the whisker rods can be obtained using the M_l value. It is known that crystalline form for tunicate is cellulose I_β,[17] for which lattice parameters were accurately determined:[18] $c = 10.36$ Å; $b = 8.17$ Å; $a = 8.01$ Å; $\gamma = 97.3°$. Cellulose chains are aligned along the c axis, which is also the longitudinal axis of the whisker. There are four glucose units by lattice (the molecular weight of each is equal to 157 g/mol), i.e., a mass of 1.076×10^{-21} g/lattice. By unit length of lattice along the c axis, this gives 1.039×10^{-22} g/(lattice Å). The number m/M_l of lattice in cross section is then deduced, i.e., 140 lattices. Therefore, the cross-sectional area of whiskers is 9162 Å^2. Assuming a circular cross section, the radius R is then calculated. Averaged over all the whisker concentrations, R is found

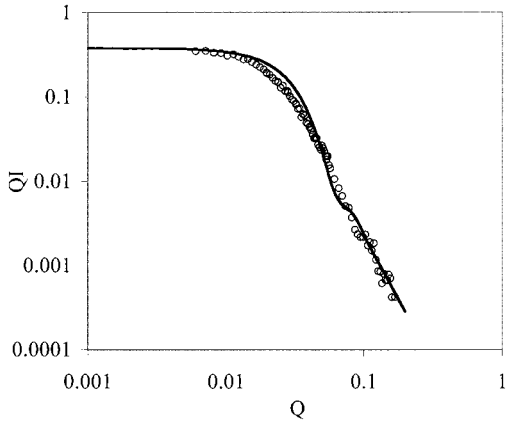

Figure 3. Experimental neutron scattering of WS02 (○) and theoretical curve calculated within the hypothesis of infinite cylinders with a radius of 60 Å. Q is in Å^{-1}, I in cm^{-1}.

to be 54 ± 2 Å. It is smaller than the value determined from the slope of the Gaussian decay (expression 2). The difference is significant, but both values (54 and 84 Å) are between 50 and 100 Å reported in the literature.[12−14]

To analyze this apparent discrepancy, a so-called Porod analysis was used with sample WS02. For scatterers with neat interfaces, relation 4 expresses the related surface per unit volume of scatterers:[19]

$$\Sigma = \frac{\lim_{Q\to+\infty} Q^4 I(Q)}{\mathrm{Inv}} \pi\phi(1-\phi) \qquad (4)$$

where ϕ is the volume fraction of scatterer and where the scattering invariant Inv is given by

$$\mathrm{Inv} = \int_0^\infty Q^2 I(Q)\, \mathrm{d}Q \qquad (5)$$

For infinite length rods $\Sigma = 2\phi/R$ and eq 4 becomes

$$R = \frac{2\mathrm{Inv}}{\lim_{q\to+\infty} (Q^4 I(Q))\pi(1-\phi)} \qquad (6)$$

The actual value of the invariant 1.5×10^{-3} cm^{-1} Å^{-3} was calculated by numerical integration within the [5×10^{-3} Å^{-1}, 2×10^{-1} Å^{-1}] Q range. The cross-sectional radius of the whiskers then deduced from eq 6 is $R_0 =$ 59 Å, which supports the validity of the calculation made from the extrapolation of M_1 value. Still, it remains the apparent discrepancy with values determined in the intermediary Q range of the Gaussian decay (values obtained from the slope of the ln(QI) vs Q^2 in Figure 5). The Q location of the disagreement is an indication that the cross-sectional shape used for the radius determination needs to be refined.

To complete the former structural analysis which takes advantage of numerical determinations performed in localized Q zones, comparisons between theoretical behavior and experimental data are considered in the whole Q range. The theoretical scattered intensity is calculated with eq 1, taking 60 Å as the radius R_0. Figure 3 shows a clear disagreement in the intermediate regime (10^{-2} Å^{-1} < Q < 10^{-1} Å^{-1}). As mentioned above, such a behavior can be indicative of a cross-sectional shape different from the assumed circular symmetry. The $R_0 =$ 84 Å value determined in the intermediate Q regime is a consequence of the inadequacy of the cross-sectional shape. Attempts to fit correctly QI as a function of Q, in both the Gaussian decay zone and that of the first oscillation observed at $Q = 0.1$ Å^{-1}, are made using expression 1. To satisfy these two constraints, it is necessary (within the hypothesis of cylindrical morphology) to consider a system with two populations of rods with different radii. Figure 4 shows the two corresponding theoretical curves for $R_0 =$ 83 Å (agreement with the Gaussian decay) and $R_0 =$ 44 Å (agreement with the oscillation at $Q = 0.1$ Å^{-1}). The visual fit allows the determination of both values with a precision of 2 Å. The quality of the fits is improved using a Gaussian distribution of the radii around these average values, defined respectively by $\epsilon = 0.1$ and $\epsilon = 0.24$ ($\epsilon = \Delta R/R_0$ at half of the Gaussian height). The intensity calculated as a volume average of these two populations, volume fractions fixed at 30% and 70%, respectively, leads to a satisfactory description of the experimental data (cf. Figure 5).

The improvement of the quality of the fit using the two-population model provides valuable indications for further attempts using a single population but with an

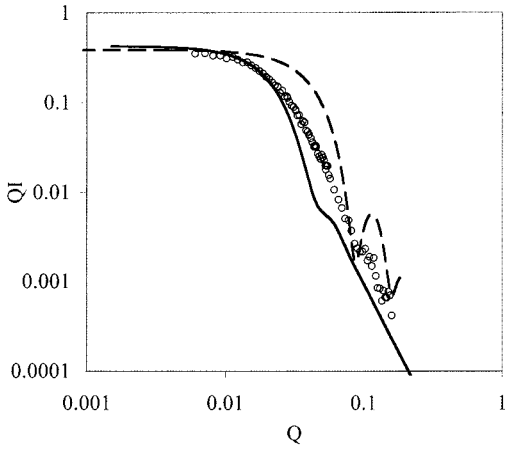

Figure 4. Experimental neutron scattering of WS02 (○) and theoretical curves calculated within the hypothesis of infinite cylinders with a radius respectively of 44 (- - -) and 83 Å (—), with a Gaussian distribution of the radius, respectively defined by $\epsilon = 0.1$ and $\epsilon = 0.24$. Q is in Å^{-1}, I in cm^{-1}. The thinner rods account for the position of the oscillation at $Q \approx 0.1$ Å^{-1} while the thicker ones describe the Gaussian intensity decrease in the intermediary Q range.

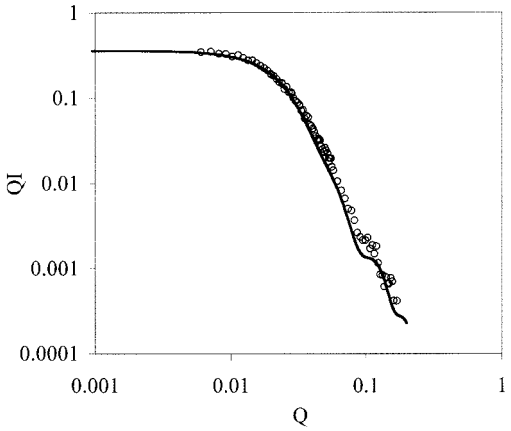

Figure 5. Experimental neutron scattering of WS02 (○) and theoretical curves calculated within the hypothesis of two populations of cylinders with a radius respectively of 44 and 83 Å, with a Gaussian distribution of the radius respectively defined by $\epsilon = 0.1$ and $\epsilon = 0.24$, and a concentration of these populations respectively equal to 30% and 70%. Q is in Å^{-1}, I in cm^{-1}.

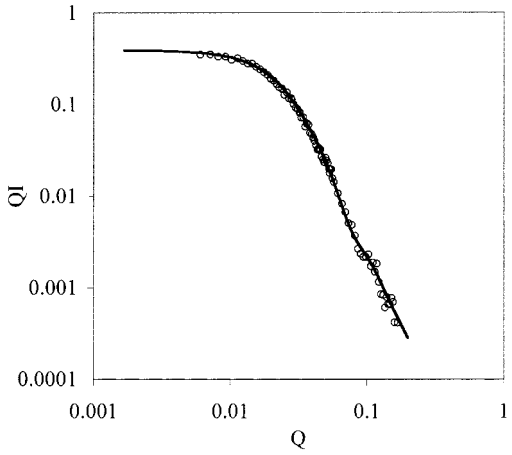

Figure 6. Experimental neutron scattering of WS02 (○) and theoretical curve calculated within the hypothesis of a rectangular section with dimensions 88 × 182 Å^2 (Gaussian distribution of the dimensions defined by $\epsilon = 0.24$). Q is in Å^{-1}, I in cm^{-1}.

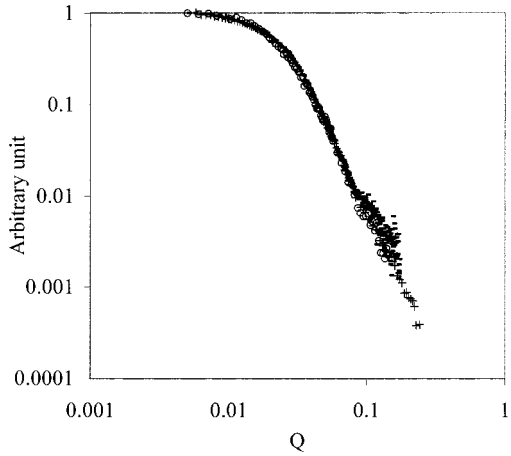

Figure 7. Comparison between neutron scattering (I.L.L. (+), L.L.B. (○)) and X-ray scattering (L.U.R.E. (—)). Q is in Å^{-1}.

appropriate anisometric cross-sectional shape. As shown in Figure 3, the discrepancy between experiment and theory in the two domains (intermediary and high Q) suggests that two different distances are concerned. Therefore, considering a rectangular section of the rodlike whiskers constitutes a logical development of the analysis. The work of Sassi[12] and Van Daele[13,14] performed by TEM also supports this hypothesis. The theoretical form factor for long rods with a rectangular ($2a \cdot 2b$) cross section is given by the expression[20]

$$I(Q) = \frac{C}{2Q}\overline{\Delta b^2} M_l \int_0^{2\pi} \left[\frac{\sin(Qa\cos\phi)}{Qa\cos\phi}\frac{\sin(Qb\cos\phi)}{Qb\cos\phi}\right]^2 d\phi \quad (8)$$

The fit to experimental curves is made taking as initial values the two characteristic dimensions 44 and 83 Å calculated previously. Figure 6 shows the fitted theoretical curves obtained with half lateral dimensions of 44 and 91 Å, with a Gaussian distribution defined by $\epsilon = 0.24$. The agreement is very satisfactory. Precision of the first value is ±1.5 Å; for the second value, the fit is less accurate and the precision is ±10 Å. Within this hypothesis, the cross-sectional area is equal to 16016 Å^2. The radius value calculated from this area (going back to the hypothesis of a circular cross-sectional area) is equal to 71 Å. This latter value is comparable to the value deduced via the invariant method (i.e., 59 Å). A definitive confirmation of these results is obtained in comparing neutron scattering data (I.L.L., L.L.B.) and SAXS data (L.U.R.E.). Figure 7 shows uniformly comparable scattering profiles. Such a behavior is an indication that the contrast for both radiations used can be modeled as a simple step function which can be considered as being monotonic at the resolution length of the experiment (ca. $2\pi/Q_{max} \approx 30$ Å).

Conclusion

The scattering investigation of aqueous suspensions of whiskers enables accurate determination of the average dimensions of the cross section of the whiskers. The analysis is performed within a concentration range where whisker interactions are absent. The small-angle scattering technique offers a great advantage compared to TEM methods, since it results from a statistical average over a large amount of whiskers in their genuine configurations (in-situ investigation).

Acknowledgment. The authors thank the Elf-Atochem Society, the ADEME, and the Ecotech program for their financial support. They also thank the neutron (I.L.L. and L.L.B.) and synchrotron facilities (L.U.R.E.) for providing radiation beams and the local contacts P. Lindner, B. Demé, J. Texeira, and P. Lesieur for their help.

References and Notes

(1) Neville, A. C. *Biology of Fibrous Composites. Development beyond the Cell Membrane*; Cambridge University Press: Cambridge, UK, 1993.

(2) Favier, V.; Chanzy, H.; Cavaille, J.-Y. *Macromolecules* **1995**, *28*, 6365.

(3) Marchessault, R. H.; Morehead, F. F.; Walter, N. M. *Nature* **1959**, *184*, 632.

(4) Nishino, T.; Takano, K.; Nakamae, K. *J. Polym. Sci., Part B: Polym. Phys.* **1995**, *33*, 1647.

(5) Tashiro, K.; Kobayashi, M. *Polym. Bull.* **1985**, *14*, 213.

(6) Tashiro, K.; Kobayashi, M. *Polymer* **1991**, *32*, 1516.

(7) Kroon-Batenburg, L. M. J.; Kroon, J.; Northolt, M. G. *Polym. Commun.* **1986**, *27*, 290.

(8) Chazeau, L.; Cavaille, J.-Y.; Dendievel, R.; Boutherin, B. *J. Appl. Polym. Sci.*, in press.

(9) Chazeau, L.; Cavaille, J.-Y.; Paillet, M. *J. Polym. Sci.*, submitted for publication.

(10) Chazeau, L.; Cavaille, J.-Y.; Perez, J. *J. Polym. Sci.*, submitted for publication.

(11) Chazeau, L.; Cavaille, J.-Y.; Terech, P. *Polymer*, in press.

(12) Sassi, J.-F.; Chanzy, H. *Cellulose* **1995**, *2*, 111.

(13) Van Daele, Y.; Gaill, F.; Goffinet, G. *J. Struct. Biol.* **1991**, *106*, 115.

(14) Van Daele, Y.; Revol, J. F.; Gaill, F.; Goffinet, G. *Biol. Cell.* **1992**, *76*, 87.

(15) Wise, L. E.; Murphy, M.; d'Addieco, A. A. *Paper Trad. J.* **1946**, *122*, 35.

(16) Guinier, A.; Fournet, G. *Small-Angle Scattering of X-rays*, Wiley & Sons: New York, 1955.

(17) Belton, P. S.; Tanner, S. F.; Cartier, N.; Chanzy, H. *Macromolecules* **1989**, *22*, 1615.

(18) Sugiyama, J.; Vuong, R.; Chanzy, H. *Macromolecules* **1991**, *24*, 4168.

(19) Porod, G. *Kolloid Z.* **1951**, *124*, 83.

(20) Mittelbach, P.; Porod, G. *J. Acta Phys. Aust.* **1961**, *14*, 185.

MA9810621